Convergence of Self-Organizing Pulse-Coupled Oscillator Synchronization in Dynamic Networks

Johannes Klinglmayr, Christian Bettstetter, *Senior Member, IEEE*, Marc Timme, and Christoph Kirst

***Abstract*—The theory of pulse-coupled oscillators provides a framework to formulate and develop self-organizing synchronization strategies for wireless communications and mobile computing. These strategies show low complexity and are adaptive to changes in the network. Even though several protocols have been proposed and theoretical insight was gained there is no proof that guarantees synchronization of the oscillator phases in general dynamic coupling topologies under technological constraints. Here, we introduce a family of coupling strategies for pulse-coupled oscillators and prove that synchronization emerges for systems with arbitrary connected and dynamic topologies, individually changing signal propagation and processing delays, and stochastic pulse emission. It is shown by simulations how unreliable links or intentionally incomplete communication between oscillators can improve synchronization performance.**

***Index Terms*—Convergence, distributed algorithms, pulse-coupled oscillators, self-organization, sensor networks, synchronization.**

I. Introduction

THE theory of pulse-coupled oscillators [1], [2], inspired by biology, offers interesting solutions for self-organizing synchronization suited for large-scale wireless ad hoc and sensor networks (see, e.g., [3]–[8] and references therein). In essence, each node of the network contains an oscillator, which changes its phase at a certain phase rate. All nodes interact with each other by exchanging pulses [4] or sync words [6], where the reception of a pulse or sync word may somehow change the oscillator's phase of the receiving node. The goal is that all nodes eventually end up in the same phase and are thus synchronized in time. The algorithm is completely flat and distributed, i.e., there is no need for selection of master nodes, as done in technologies like Bluetooth.

Almost all work on the application of pulse-coupled oscillators to real world systems is based on simulations, where the performance of a particular modification or extension of the Mirollo–Strogatz coupling scheme [2] is evaluated in terms of time-to-synchrony and synchronization precision as a function of network parameters. Analytical results on pulse-coupled oscillators can be found in physics and other natural sciences. These results are often based on simplifying assumptions, which restrict their application to real world networks [2], [7], [9]–[13]. They do not include at least one of the following conditions: random individual pulse delays, unreliable links or pulse emission, or nonfully connected and dynamic networks. Hence, for applications in real world wireless environments, theoretical results from other disciplines often cannot be used.

In this paper, we describe a method that proves to achieve full synchronization under a wide range of system environments, which narrows the gap to real world settings. We provide four main contributions: First, by addressing all conditions mentioned above simultaneously the proof we provide here substantially backs the fundamentals for applications. Second, while natural synchronization bounds exist, which state that nodes cannot align their internal clocks better than the uncertainty in the transmission delay [14], [15], our proposed algorithm shows to converge to fully synchronized oscillations in the presence of arbitrarily distributed propagation delays if there is a nonzero probability for minimal transmission times. Third, we show that a reduction of the number of transmissions, which are already minimized in duration to pulses, further improves the efficiency for synchornization. Fourth, for specific networks, unreliable links between oscillators improve synchronization performance [16]–[18]. These achievements are due to the specific design of the coupling strategy: We combine refractory, negative, and positive phase coupling together with stochastic pulse emission [18]–[22].

This paper considerably extends and generalizes the work in [18] published by the same authors in a physics journal. Major differences are as follows: We generalize our proof to systems which are closer to the real world taking into account that instantaneous pulse transmissions are impossible and that network links can dynamically change in time. Our generalizations include the special case of zero communication delay and fixed network topologies as in [18]. Including nonzero minimal transmission delays required a new class of update functions [compare [18] with (6)], and the introduction of new mathematical concepts as the complexity of the analysis has

Manuscript received December 4, 2015; revised December 11, 2015 and June 9, 2016; accepted July 1, 2016. Date of publication July 20, 2016; date of current version March 27, 2017. This work was supported by FFG Austria under FIT-IT Grant 825893 (ROSSY), by Lakeside Labs GmbH with funding from ERDF/BABEG/KWF under Grant 20214/23794/35530 (HiSONS), by the Linz Center of Mechatronics (LCM) in the framework of COMET-K2, by a Grant of the Federation of Carinthian Industry (IV) to JK, by a Grant by the Federal Ministry of Education and Research (BMBF) Germany under Grant 01GQ1005B, and by the Max Planck Society, both to MT, and a Fellowship from the Rockefeller University to CK. Recommended by Associate Editor V. Gupta.

J. Klinglmayr is with Linz Center of Mechatronics GmbH, 4040 Linz, Austria, and also with the University of Klagenfurt Max-Planck Institute Göttingen.

C. Bettstetter is with the University of Klagenfurt, Institute of Networked and Embedded Systems, Lakeside Labs GmbH, 9020 Klagenfurt, Austria (e-mail: johannes.klinglmayr@lcm.at).

M. Timme is with the Max Planck Institute for Dynamics and Self-Organization (Head, Network Dynamics), Bernstein Center for Computational Neuroscience Göttingen, Institute for Nonlinear Dynamics, Faculty of Physics, University of Göttingen, 37077 Göttingen, Germany.

C. Kirst is with Rockefeller University, New York, NY 10065 USA.

Color versions of one or more of the figures in this paper are available online at http://ieeexplore.ieee.org.

Digital Object Identifier 10.1109/TAC.2016.2593642

significantly increased (cf., e.g., example 3 and Lemmata 1, 2, 5–11). Moreover, time varying network topologies required additional analysis (cf., e.g., Lemma 9) in which we derive precise analytic conditions on the dynamics of the network structure under which synchronization is still guaranteed. We further provide analytic estimates for the speed of synchronization (see Section IV) and also explicitly study the robustness of our method and its resilience to environments for which the system is not designed for (see Section V).

The article is structured as follows: In Section II we give background information, define the setting, and present the individual dynamics. In Section III the main synchronization proof is given, which is divided into two parts. First, we show that in an invariant subspace, defined via a synchronization condition, the phases of all oscillators synchronize. Second, we show that every initial condition will eventually fulfill the synchronization condition. In Section IV we give estimates on the speed of the synchronization process, and in Section V we support our theoretical results by simulations and demonstrate fast convergence times, robustness and efficiency. Finally, we conclude in Section VI.

II. Pulse-Coupled Oscillators

A. Background and Related Work

Pulse-coupled oscillators (PCO) have been used for several decades to model synchronization phenomena found in nature, especially the synchronous flashing of fireflies [1], [23], [24].

The coupling between oscillators in a PCO network is captured by an update function which determines the oscillator's phase change upon reception of a pulse. This function can have phase advancing (excitatory) [2] or phase retarding (inhibitory) effects [25], or employs a combination of both [18].

The basis of recent work on pulse-coupled oscillators is the work by Mirollo and Strogatz [2]. They analyze a set of identical all-to-all coupled oscillators in a delay-free environment and prove that all oscillators synchronize from almost all initial phase positions using excitatory coupling. Follow-up research takes into account more general modeling assumptions. For example, delays in the system have desynchronizing effects, but these effects can be overcome by proper design of the update function, e.g., by using "refractory" periods (see [3], and [26]–[28]). The effects of inhibitory coupling or its interaction with excitatory coupling are studied in [29]–[33].

The application of pulse-coupled oscillators for distributed synchronization in computer and communication networks is described, e.g., in [3]–[7], [34], and [35]. The results of these papers are, however, mainly based on simulations and implementations or restricted to the theory of two oscillators. In contrast to PCO models for biological systems, technical systems provide the freedom of choosing coupling strategies detached from biological constraints. In this respect different artificial coupling schemes show beneficial and remarkable effects, as they provide synchronization for specific environments (see [18], [20], [21], [25], and [36]).

The presented article studies the asymptotic oscillator behavior with the help of a *synchronization condition*. In the related field of continuous phase coupled oscillators systems, for example contraction theory uses a comparable methodology (e.g., [37]–[43]). However, most results and analysis methods on continuous coupling are currently not applicable for pulse-coupled oscillator systems due to the discrete nature of the interaction [43].

B. System Setting

Work on synchronization for PCOs started with idealized conditions such as all-to-all networks or instant transmissions [1], [2]. To better match the theory with technical applications, coupling specifications were studied. For instance, windows without phase changes (so called "refractory" periods [26]), or hybrid coupling (positive and negative coupling, e.g., [19], [36]) were introduced. These modifications allowed to obtain synchronization statements while generalizing system requirements. Here, we continue this approach. We present a certain class of coupling and show its synchronization behavior under the so far largest set of simultaneous constraints that can arise in real world systems. We first introduce the system setting and then study its dynamics and behavior.

1) Network: Consider a set of N oscillators indexed by $i \in I := \{1, 2, \dots, N\}$. The connections between the oscillators at a given time t are given by on a directed graph $\mathcal{G}(t)$. The graph can vary over time. $\mathcal{G}(t)$ is allowed to be disconnected from time to time, but is assumed to be strongly connected for an infinite number of time intervals of at least a duration of $\sigma_{\mathcal{G}} > 0$. At time t, we define the predecessors $\mathtt{pre}_i(t)$ as the set of oscillators that have a directed link to oscillator i. Accordingly, the set of all oscillators that oscillator i has a directed link to are called successors $\mathtt{suc}_i(t)$. Note that $\mathtt{pre}_i(t)$ and $\mathtt{suc}_i(t)$ may change over time. For a subset $S \subset I$ of oscillators and for a point in time $t \geq 0$ (or a time interval T), the set of all predecessors $\mathtt{pre}_S(t)$, $(\mathtt{pre}_S(T))$ of S is defined by

$$\mathtt{pre}_S(t) := \cup_{k\in S}\mathtt{pre}_k(t),\ \mathtt{pre}_S(T) := \cap_{t\in T}\mathtt{pre}_S(t). \quad (1)$$

A similar definition applies for $\mathtt{suc}_S(t)$ and $\mathtt{suc}_S(T)$.

2) Oscillators: Each oscillator $i \in I$ is determined by a phase $\phi_i(t) \in [0, 1]$, that changes with constant rate

$$\frac{d}{dt}\phi_i = 1 \quad (2)$$

see, e.g., [2], [20], [36], and [44]. Upon passing the threshold 1, the oscillator resets its phase to 0, i.e.,

$$\phi_i(t) = 1 \Rightarrow \phi_i(t^+) = \lim_{s\searrow 0} \phi_i(t + s) = 0 \quad (3)$$

as in [2], [20], [31], [36], and [44] and emits a pulse with an emission probability $p_{\text{send}} \in (0, 1)$, compare [16]. The time at which the mth pulse of oscillator i is emitted is called t_m^i. Considering the network of all oscillators we denote t_n as the time of the nth pulse in the entire network.

3) Delays: A pulse emitted by oscillator i at time t_n experiences a delay τ_{ij}^n until it is received by oscillator $j \in \mathtt{suc}_i([t_n, t_n + \tau_{ij}^n])$. The delay is distributed in the interval $[\tau_{\min}, \tau_{\max}]$, where $\tau_{\min} \geq 0$ is the minimal and $\tau_{\max}$ the

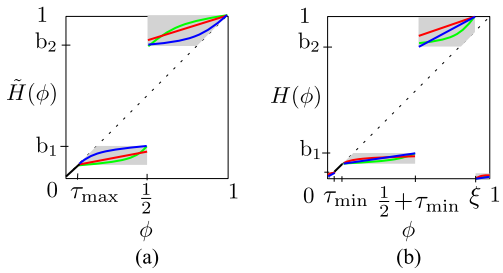

Fig. 1. Examples of the functions in (6) and (7) that lead to synchrony. (a) Auxiliary function $\tilde{H}(\phi)$ with $b_1 = (1/4) - \tau_\Delta$ and $b_2 = (3/4) + \tau_\delta$. (b) Update function $H(\phi)$ with $b_1 = (1/4) - \tau_{\max}$ and $b_2 = (3/4) + \tau_{\max}$. Each color represents one coupling function.

maximum possible delay. We assume that delays arbitrarily close to $\tau_{\min}$ occur repeatedly: In other words, the probability for delays occurring in arbitrary small intervals that include $\tau_{\min}$ are positive $\mathbb{P}[\tau \in [\tau_{\min}, \tau_{\min} + \varepsilon]] > 0$ for all $\varepsilon > 0$. For technical reasons [see requirements on (7)] we demand $2\tau_{\max} + \tau_{\min} < (1/4)$ and $\tau_{\max} < (1/8)$.

We further define

$$\tau_\delta := \tau_{\max} - \tau_{\min} \text{ and } \tau_\Delta := \tau_{\max} + \tau_{\min}. \tag{4}$$

The reader will notice the technical restrictions on the delay. Section III-E will show that these are the most general conditions for the presented coupling to achieve synchronization.

We allow for $\tau_{\min} \geq 0$ since delays cannot be arbitrarily small in technical systems. This is one important difference to [18], where $\tau_{\min} = 0$ was required for analytic tractability.

4) Coupling: Whenever an oscillator j receives a pulse from oscillator i and is not resetting at the same time, it performs a phase update according to

$$\phi_j\left(t_n + \tau_{ij}^{n+}\right) = H\left(\phi_j\left(t_n + \tau_{ij}^{n}\right)\right) \tag{5}$$

where $H(\cdot)$ is the phase update function (equivalently called coupling function) [7]. We set

$$H(\phi) = \tilde{H}(\phi - \tau_{\min} \mod 1) + \tau_{\min} \mod 1 \tag{6}$$

with auxiliary function [18]

$$\tilde{H}(\phi) = \begin{cases} \phi & \phi \leq \tau_{\max} \\ h_1(\phi) & \tau_{\max} < \phi \leq \frac{1}{2} \\ h_2(\phi) & \frac{1}{2} < \phi \leq 1 \end{cases} \tag{7}$$

where the functions $h_1(\phi)$ and $h_2(\phi)$ are smooth and satisfy $0 < (dh_1/d\phi) < 1$ and $0 < (dh_2/d\phi) < 1$; $h_1(\tau_{\max}) = \tau_{\max}$, $h_1(1/2) \leq (1/4) - \tau_\Delta$; and $h_2((1/2)^+) \geq (3/4) + \tau_\delta$, $h_2(1) = 1$. We abbreviate $\xi := \lim_{x \nearrow 1} H^{-1}(x)$. Examples are shown in Fig. 1.

Note that the restrictions on h_1 and h_2 are less constraining than those in [18] if $\tau_{\min} = 0$, which thus generalizes the results in [18] further.

An oscillator is said to *adjust*, if it updates its phase such that $\phi(t^+) \neq \phi(t)$ upon receiving a pulse at time t. The adjustment is called inhibitory if $\phi(t) \in (\tau_\Delta, (1/2) + \tau_{\min}] \cup (\xi, 1]$ such that $\phi(t^+) < \phi(t)$ and excitatory if $\phi \in (0, \tau_{\min}) \cup ((1/2) + \tau_{\min}, \xi]$ such that $\phi(t^+) > \phi(t)$. The phase interval $[\tau_{\min}, \tau_\Delta]$ with no adjustments at pulse reception, i.e., $\phi(t^+) = \phi(t)$, is called *refractory period*.

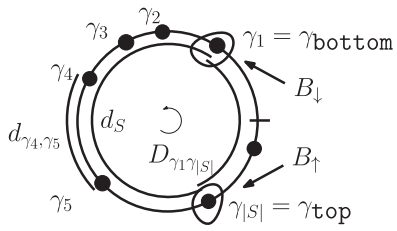

Fig. 2. Definitions. Examples of d_{ij}, γ_i, d_S, D_{ij}, $\gamma_{\texttt{top}}$ and $\gamma_{\texttt{bottom}}$, for a set $S := \{\gamma_1, \gamma_2, \ldots, \gamma_{|S|}\}$.

Below, we prove that the network dynamical system (2), (3), (5) for the class of coupling functions (6), (7) implies synchrony of all oscillators from arbitrary initial conditions with probability 1.

C. Distances and Boundary Sets

The oscillators can be represented as dots moving counterclockwise on a circle with circumference 1 (see Fig. 2). The *natural circular distance* is defined by

$$d_{ij} := d(\phi_i, \phi_j) := \min\left(|\phi_i - \phi_j|, 1 - |\phi_i - \phi_j|\right). \tag{8}$$

To simplify the formalism we introduce an interval notation between two points ϕ_i and ϕ_j on the circle by setting

$$[\phi_i, \phi_j)_1 := \begin{cases} [\phi_i, \phi_j) & \text{if} \quad \phi_i \leq \phi_j \\ [0,1] \setminus [\phi_j, \phi_i) & \text{if} \quad \phi_i > \phi_j \end{cases} \tag{9}$$

and analogous for closed and open intervals.

Additionally, let D_{kj} denote the smallest phase interval on the circle from ϕ_k to ϕ_j, i.e., if $\phi_k < \phi_j$ then

$$D_{kj} := \begin{cases} [\phi_k, \phi_j] & \text{if } \phi_j - \phi_k \leq \frac{1}{2} \\ [\phi_j, \phi_k]_1 & \text{if } \phi_j - \phi_k > \frac{1}{2} \end{cases} \tag{10}$$

and if $\phi_j < \phi_k$ then

$$D_{kj} := \begin{cases} [\phi_j, \phi_k] & \text{if } \phi_k - \phi_j \leq \frac{1}{2} \\ [\phi_k, \phi_j]_1 & \text{if } \phi_k - \phi_j > \frac{1}{2} \end{cases}. \tag{11}$$

Note that by this definition we have $d_{ij} = \mu(D_{ij})$ where μ is the uniform Lebesgue measure on the circle.

For an index subset $S \subset I$, we define its *outer edge set* via $\partial S(t) := \{i \in S : \exists j \notin S \text{ s.t. } j \in \texttt{suc}_i(t)\}$. These are all the nodes in S with a link to nodes outside of S at time t.

For any $S \subset I$ we define the *diameter* of S via

$$d_S := 1 - \max_{i=1,\ldots,|S|} \begin{cases} \phi_{\gamma_{i+1}} - \phi_{\gamma_i} & \text{for } i < |S| \\ 1 - \phi_{\gamma_i} + \phi_{\gamma_1} & \text{for } i = |S| \end{cases} \tag{12}$$

where γ_i, $i \in \{1, \ldots, |S|\}$ is an index permutation such that $\phi_{\gamma_i} \leq \phi_{\gamma_{i+1}}$ for all i.

We further set $\texttt{top} = i^*$ and $\texttt{bottom} := (i^* \mod |S|) + 1$ if i^* is an index that yields the maximum in the expression in (12).

The *boundary sets* that give rise to the diameter in (12) are defined as

$$B_\uparrow(t) := \left\{j \in I : \phi_j(t) = \phi_{\gamma_{\text{top}}}(t)\right\} \tag{13}$$
$$B_\downarrow(t) := \left\{j \in I : \phi_j(t) = \phi_{\gamma_{\text{bottom}}}(t)\right\}. \tag{14}$$

These concepts are illustrated in Fig. 2 [see also Fig. 4(a) where we have $j \in B_\uparrow$ and $k \in B_\downarrow$ and Fig. 4(d) for $k \in B_\uparrow$ and $j \in B_\downarrow$ and Fig. 5(a) for examples of D_{ij}].

III. Proof of Convergence

For the introduced class of update functions, we now show their synchronizing effect on the oscillators: We first identify a contracting subset which eventually leads to synchrony and then we show that this set is a global stochastic attractor, i.e., every set of initial conditions will eventually reach this contracting subset with probability 1.

A. Proof Outline

We prove that any PCO system with dynamics as defined in (2)–(7) synchronizes with probability 1. This proof is made in two main steps. First, in Section III-C, we identify a condition on the diameter d_I of all oscillators I and show that once this condition holds at time point t_*, it will hold for all future times $t \geq t_*$. Moreover, we show that $d_I(t) \leq d_I(t_*)$ and employing stochastic pulse emission that $d_I(t)$ reaches 0 with probability 1, i.e., the fully phase-synchronized state is an attractor of the stochastic dynamics. Second, in Section III-D, we show that the condition on the diameter d_I will be met at some point in time with probability 1. We prove this by constructing a sequence of events that leads to the synchronization condition and show that this sequence occurs with positive probability at any reception event, i.e., the synchronized state is a global stochastic attractor of the system.

Previously [18], we assumed that arbitrary short delays occur with nonzero probability. We now consider minimal delays that are nonzero and can vary over time. As a consequence, we need to design a more general update function (6) as compared to [18]. This alters the analytic proof substantially, requiring, e.g., the introduction of boundary sets (used in Lemmata 6–9), and a different treatment of the effect of phase updates on the various distance measures with a large variety of subcases (Lemmata 1, 2, 5–11). Moreover, we here also allow for time varying directed topologies. This again alters the convergence proof substantially and reveals conditions on the dynamics of the network topology necessary for synchronization (see, e.g., Lemma 9).

B. Four Lemmata

Lemma 1: The update function $H(\cdot)$ from (6) determines five *update intervals* U_k, $k \in \{1, \ldots, 5\}$ for the phases, such that if oscillator j receives an incoming pulse at time t and $\phi_j(t) \in U_k$, the updated phase $\phi_j(t^+)$ has the following properties (see also Fig. 3):

- $U_1 := (0, \tau_{\min})$, excitatory phase jumps, $\phi_j(t) < \phi_j(t^+) < \tau_{\min}$ and $\phi_j(t^+) \in U_1$;

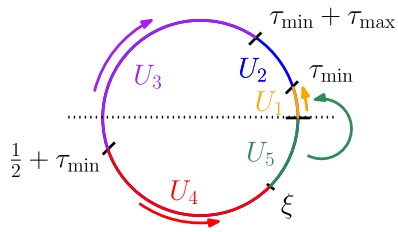

Fig. 3. The update intervals for the different phases. Within each update interval the phase adjustment is either inhibitory (U_3, U_5), excitatory (U_1, U_4) or refractory (U_2).

- $U_2 := [\tau_{\min}, \tau_\Delta]$, no phase jumps, $\phi_j(t^+) = \phi_j(t)$ and $\phi_j(t^+) \in U_2$;
- $U_3 := (\tau_\Delta, (1/2) + \tau_{\min}]$, inhibitory phase jumps, $\tau_\Delta < \phi_j(t^+) < \phi_j(t)$ and $\phi_j(t^+) \leq (1/4) - \tau_{\max}$, hence $\phi_j(t^+) \in U_3$;
- $U_4 := ((1/2) + \tau_{\min}, \xi)$, excitatory phase jumps, $\phi_j(t) < \phi_j(t^+)$, $\phi_j(t^+) \geq (3/4) + \tau_{\max}$ and $\phi_j(t^+) \in U_4 \cup U_5$;
- $U_5 := [\xi, 1)$, inhibitory phase jumps, $\phi_j(t^+) < \phi_j(t)$ and $\phi_j(t^+) \in U_1$.

Proof: The properties follow directly from the definition of $H(\cdot)$ in (6) via the stepwise definition of $\tilde{H}(\cdot)$ from (7) and the modulo operation used in (6), compare Fig. 1. ■

Lemma 2: If at some time t', oscillator i is at the threshold with $\phi_i(t') = 1$, then for all $t \in (t', t' + \tau_{\max}]$, $\phi_i(t) \in [0, \tau_\Delta]$ and for all $t \in (t' + \tau_{\min}, t' + \tau_{\max}]$, $\phi_i(t) \in U_2$.

Proof: Take a time t' and an oscillator i such that $\phi_i(t') = 1$. Then oscillator i will reset and we have $\phi_i(t'^+) = 0$. If oscillator i will not receive a signal within $(t', t' + \tau_{\max}]$, we have for all $t \in (t', t' + \tau_{\max}]$, $\phi_i(t) \leq \tau_{\max}$, due to (2). If there is a reception event at some time t_r, we see that ϕ_i passes through U_1 and U_2. U_1 can only cause positive phase jumps, see Lemma 1. Thus the minimum phase that oscillator i attains at $t' + \tau_{\min}$ and at $t' + \tau_{\max}$ is bounded from below by $\phi_i(t' + \tau_{\min}) = \tau_{\min}$ and $\phi_i(t' + \tau_{\max}) = \tau_{\max}$. For an upper bound, larger phases are obtained if phase updates occur within U_1. Therefore, the maximum phase achievable is $\phi_i(t'^+) = \tau_{\min}$ and due to the refractory period and (2) $\phi_i(t' + \tau_{\max}) = \tau_{\min} + \tau_{\max}$. ■

Corollary 1: Whenever a signal is received at some t_r, there is an oscillator i with $\phi_i(t_r) \in U_2$.

Proof: If an oscillator j receives a signal at t_r, there has to be some oscillator i that emitted the signal and reset at $t' \in [t_r - \tau_{\max}, t_r - \tau_{\min}]$ and we can apply Lemma 2. ■

Lemma 3: For all pairs of oscillators $(i, j) \in I^2$, any distance d_{ij} only changes due to a reception event.

Proof: At any point in time t', one of the following situations occurs: (a) none of the oscillators receives a pulse; (b) at least one oscillator receives a pulse. Assuming (a), due to the uniform phase shift (2) and the circular definition of distance (8) there are no changes in distance. This also includes situations where oscillators reset. Hence, if a distance between oscillators changes it has to change via (b). ■

Corollary 2: The boundary sets do not change unless a reception event happens.

Proof: This is a direct consequence of Lemma 3. Distances are defined via phase positions as are boundary sets. Hence they can only change if distances change. ■

Lemma 4: For every oscillator $i \in I$, the time of its nth fire event is finite almost surely, i.e.,

$$\mathbb{P}\left[t_n^i < \infty\right] = 1. \tag{15}$$

Proof: We first show that every oscillator resets an arbitrary number of times: Assume there is an oscillator i that does not reset arbitrarily often. Then there has to be a time t' from which on it does not reset anymore. Since (2) holds for oscillator i, this can only be achieved by repeated pulse receptions that retard ϕ_i. As the frequency of each oscillator, i.e., the number of resets it experiences per time, is bounded (cf. [45]), oscillator i receives only a maximum finite number M of pulses within a unit time interval. As the probability of emission of each pulse is $p_{\text{send}} < 1$, oscillator i is retarded in a unit time interval with some probability of at most some $\zeta < 1$. Thus, the probability that i is repeatedly retarded for m subsequent unit time intervals is at most ζ^m, which tends to zero as $m \to \infty$. Hence, oscillator i reaches threshold and resets within some finite time, yielding

$$\mathbb{P}\left[\phi_i(t) < 1,\ \forall t \geq t'\right] = 0. \tag{16}$$

Thus, oscillator i resets arbitrarily often and emits a pulse with probability p_{send} whenever it resets. The probability of m resets of i not emitting a pulse is $(1-p_{\text{send}})^m$, and thus t_n^i is finite with probability 1. ■

C. Synchronization Condition

An essential building stone for guaranteeing synchronization is the use of a specific class of system states. It is defined via the *synchronization condition* as follows.

We say that at a time t_* the synchronization condition holds if

$$d_I(t_*) \leq \frac{1}{2} - \tau_{\max}. \tag{17}$$

Let us note the following consequences:

Lemma 5: If the synchronization condition (17) holds, then for any pair $(j,k) \in I^2$ and an oscillator $i \in I$ that "lies in between" oscillators j and k (cf. Fig. 4), i.e., for which

$$\phi_i \in D_{jk} \tag{18}$$

we have $D_{jk} = D_{ji} \cup D_{ik}$ and thus

$$d_{jk} = d_{ji} + d_{ik}. \tag{19}$$

Proof: D_{jk} is the smallest interval on the circle from k to j. Take $b_\downarrow \in B_\downarrow$ and $b_\uparrow \in B_\uparrow$ then $\mu(D_{b_\downarrow b_\uparrow}) = d_I < (1/2)$ due to (17). Moreover, by definition of the diameter we must have $\phi_k, \phi_j \in D_{b_\downarrow b_\uparrow}$ and therefore also $D_{jk} \subset D_{b_\downarrow b_\uparrow}$, i.e., $d_{jk} = \mu(D_{jk}) < 1/2$. As $\phi_i \in D_{jk}$ we thus must have $D_{ji} \cup D_{ik} = D_{jk}$ and $D_{ji} \cap D_{ik} = \{\phi_i\}$. Hence also $d_{jk} = \mu(D_{jk}) = \mu(D_{ji}) + \mu(D_{ik}) = d_{ji} + d_{ik}$. ■

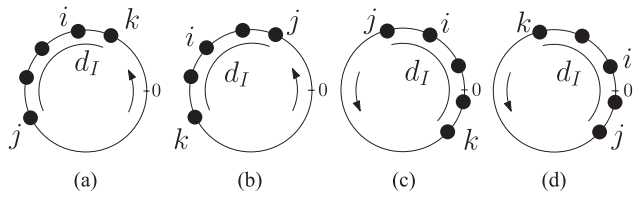

Fig. 4. Representation of oscillators on a circle. Four different arrangements of oscillators. In all four situations oscillator i is "in between" oscillator j and k, see (18).

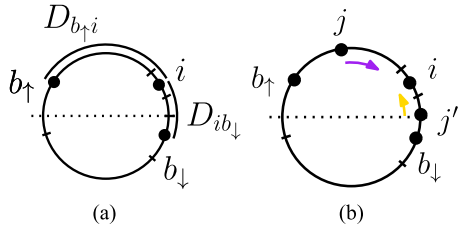

Fig. 5. An example for a phase adjustment as considered in lemma 7. (a) If d_I fulfills the synchronization condition (17) then at a reception event at time t_r there is an oscillator i with phase in U_2, $d_I = D_{b_\uparrow i} \cup D_{ib_\downarrow}$. (b) If at t_r an oscillator j or j' receives a signal, it adjusts according to lemma 1, indicated by the colored arrows, and moves closer to i. In particular, this holds for oscillators in the boundary sets.

Lemma 6: If (17) holds, then at any reception event at time $t_r \geq t_*$, for all $j \in B_\uparrow(t_r)$ we have $\tau_{\min} \leq \phi_j(t_r) \leq (1/2) + \tau_{\min}$.

Proof: Let us assume an oscillator j receives a signal at time t_r with $j \in B_\uparrow(t_r)$, and (17) holds. Due to Corollary 1 we have an oscillator i that emitted the corresponding signal and $\phi_i(t_r) \in [\tau_{\min}, \tau_\Delta]$. Let us now consider the extreme scenarios, when $\phi_j(t_r)$ is smallest or largest. If $\phi_j(t_r)$ is smallest, then $\phi_j(t_r) = \phi_i(t_r) \geq \tau_{\min}$. If $\phi_j(t_r)$ is largest, then $d_I(t_r) = (1/2) - \tau_{\max}$ holds, and $\phi_i(t_r) = \tau_\Delta$. Then we have for oscillator j

$$\tau_{\min} \leq \phi_j(t_r) \leq \tau_\Delta + \frac{1}{2} - \tau_{\max} = \frac{1}{2} + \tau_{\min}. \tag{20}$$

■

We now identify a key observation for the proof of synchronization: The diameter does not increase when the synchronization condition holds.

Lemma 7: If (17) holds at time t_* then for all $t \geq t_*$ we have

$$d_I(t) \leq d_I(t_*). \tag{21}$$

Proof: Due to Lemma 3, a change in the diameter is only possible via a reception event. Thus, consider such an event at time $t_r \geq t_*$ in which oscillator j receives a pulse generated at time t_e by oscillator i. By Lemma 2 we have $\phi_i(t_r) \in U_2$ and thus by Lemma 1 $\phi_i(t_r^+) = \phi_i(t_r)$. Take $b_\uparrow \in B_\uparrow(t_r)$ and $b_\downarrow \in B_\downarrow(t_r)$. Using the synchronization condition (17) and Lemma 5 we have $\phi_j(t_r) \in D_{b_\uparrow b_\downarrow}(t_r)$ and also $D_{b_\uparrow b_\downarrow}(t_r) = D_{b_\uparrow i}(t_r) \cup D_{ib_\downarrow}(t_r)$, see Fig. 5(a). Hence either $\phi_j(t_r) \in D_{b_\downarrow i}(t_r)$ or $\phi_j(t_r) \in D_{ib_\uparrow}(t_r)$. Moreover, again using the synchronization condition (17) and $\phi_i(t_r) \in U_2$ we conclude $D_{b_\uparrow i}(t_r) \subset U_2 \cup U_3$ and $D_{ib_\downarrow} \subset U_4 \cup U_5 \cup U_1 \cup U_2$. Using Lemma 1 we have: in the former case, $\phi_j(t_r) \in U_2 \cup U_3$ and $\phi_j(t_r^+) \in U_2 \cup U_3$,

in the latter case, $\phi_j(t_r) \in U_4 \cup U_5 \cup U_1 \cup U_2$ and $\phi_j(t_r^+) \in U_4 \cup U_5 \cup U_1 \cup U_2$. Applying the phase update statements from Lemma 1 we arrive at $d_{ij}(t_r^+) \leq d_{ij}(t_r)$ in both situations, see Fig. 5(b). As other distances do not change we have for all $k \in I$, $d_{ik}(t_r^+) \leq d_{ik}(t_r)$ and using Lemma 5 with $j \in B_\uparrow(t_r^+)$ and $k \in B_\downarrow(t_r^+)$ we arrive at (21). ■

For the arguments in Lemma 7 the properties of the phase updates as described in Lemma 1 are crucial. This motivates the specific design of the update function.

We now show that eventually the diameter d_I decays to zero, by first showing in the next two lemmata that the boundary sets almost surely lose elements if the diameter stays constant.

Lemma 8: If (17) holds and for all $t \geq t_*$ the diameter $d_I(t) = c > 0$ stays constant the boundary sets $B_\downarrow$ and $B_\uparrow$ can only lose elements, i.e., for all $t \geq t_*$, $B_\downarrow(t) \subset B_\downarrow(t_*)$ and $B_\uparrow(t) \subset B_\uparrow(t_*)$.

Proof: By Lemma 3 the boundary sets can only change during a reception event at time t_r. By Lemma 2 there is an oscillator i with $\phi_i(t_r) \in U_2$ and thus by Lemma 1 $\phi_i(t_r^+) = \phi_i(t_r)$. By the same argument as in Lemma 7 we have $\phi_k(t_r^+) \leq \phi_k(t_r)$ for all $k \in B_\uparrow(t_r)$ and thus $B_\uparrow(t_r^+)$ can only contain oscillators $j \notin B_\uparrow(t_r)$ if for all oscillators $k \in B_\uparrow(t_r)$, $\phi_k(t_r^+) < \phi_k(t_r)$, such that $\phi_j(t_r^+) \geq \phi_k(t_r^+)$. Via the same arguments used in Lemma 7 we further conclude that for all $l \in I$ the distances to i do not increase, i.e., $d_{il}(t_r^+) \leq d_{il}(t_r)$. This in total implies a decrease in the diameter $d_I(t_r) < d_I(t_r^+)$ in contradiction to our assumption of constant d_I. We arrive at a similar contradiction when considering $B_\downarrow$. ■

Lemma 9: If (17) holds and for all $t \geq t_*$ the diameter $d_I(t) = c > 0$ stays constant the boundary sets $B_\downarrow$ and $B_\uparrow$ will lose elements with probability one.

Proof: We construct a line of events in which $B_\downarrow$ loses an element and show that it has positive probability. Therefore, consider a time $t' \geq t_*$ in which the following conditions hold:

1) The network topology is constant in the time interval $T_G = [t', t'']$ of length $t'' - t' \geq \sigma_G > 0$. By assumption on the dynamics of the network structure this event has positive probability (cf. Section II-B1).
2) Set $B_\downarrow(T_G) := \cap_{t \in T_G} B_\downarrow(t)$. Then using the definition from (14), $B_\downarrow(t)$ is never empty and by Lemma 8 $B_\downarrow(T_G)$ is also non empty. Due to 1.) and the assumption that the network is strongly connected we have that $\mathtt{pre}_k(T_G)$ is non empty for all $k \in B_\downarrow(T_G)$. Moreover, as the diameter is positive, $d_I > 0$, and again due to the strongly connectedness of the network there is a $k \in B_\downarrow(T_G)$ and $i \in \mathtt{pre}_k(T_G)$ and $\epsilon > 0$ such that $d_{ik}(t') = \varepsilon > 0$.
3) We choose oscillators k and i as in 2.) and assume that i emitted a pulse at some time $t_e \leq t'$ which is received at time $t_r \in [t_e + \tau_{\min}, t_e + \tau_{\min} + \varepsilon] \cap T_G$ by oscillator k. By Lemma 4 and using the assumption that delay times arbitrary close to the lower bound $\tau_{\min}$ have positive probability this event in total has positive probability, see Figs. 6 and Fig. 7 for illustration.

Analog to the reasoning in Lemma 7 we have $\phi_k(t_r) \notin U_3$ and hence $d_{ik}(t_r^+) < d_{ik}(t_r)$. By assumption the diameter stays constant and by using Lemma 8 this is only possible if $k \notin B_\downarrow(t_r^+)$, i.e., $B_\downarrow(t_r^+)$ has lost at least one element. ■

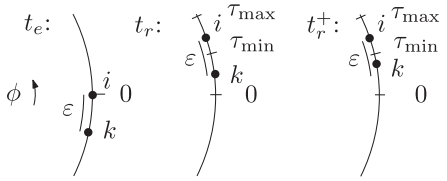

Fig. 6. A zoom onto the circle around 0. We show an example for the phase update as in lemma 9.

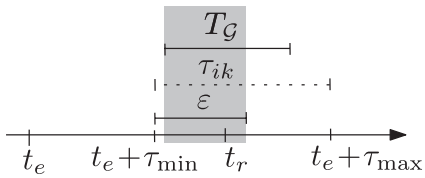

Fig. 7. Example of a time line according to the construction of conditions in lemma 9 that lead to a decrease in the size of the boundary set. The gray shaded area indicates the time window in which there is a positive probability to decrease the distance between the two oscillators i and k.

Lemma 10: If (17) holds, then

$$\mathbb{P}\left[\lim_{t\to\infty} d_I(t) > 0\right] = 0. \tag{22}$$

Proof: Assume (22) does not hold. Since Lemma 7 holds, there is a t' such that for all $t > t'$ we have $d_I(t) = c$. If so, Lemma 8 says $|B_\downarrow(t)|$ cannot increase with time, and Lemma 9 says it decreases with positive probability, which means $|B_\downarrow(t)|$ vanishes with time which is a contradiction to its definition in (14). Hence (22) has to hold. ■

D. Inevitable Synchronization

So far we showed, that synchrony is achieved if the synchronization condition holds. We now show that the synchronization condition is always reached with probability 1 for all initial conditions:

Lemma 11: There is a time t_* with $0 \leq t_* < \infty$ such that

$$\mathbb{P}\left[d_I(t_*) \leq \frac{1}{2} - \tau_{\max}\right] > 0. \tag{23}$$

Proof: Assume at time t', (17) does not hold for I. We define a subset $S \subset I$ with $d_S(t') \leq (1/2) - \tau_{\max}$. In the following, we show that there is a positive probability that for some $t'' \geq t'$, $S(t'') = I$ is achieved: Take $S \neq \emptyset$. As $d_S(t') = 0$ for $S = \{i\}$, $i \in I$, this is always possible. For any finite time interval T_S, there is a positive probability that no pulse from $\mathrm{pre}_S(T_S) \setminus S$ is received by all members of S, since $p_{\mathrm{send}} < 1$. For that time we can then consider the oscillators in S as a subnetwork not receiving any pulses from the oscillators in the complement of S, and thus for this subnetwork (17) applies. Therefore Lemma 10 applies and there is a positive probability that for some $t'' > t'$, $d_S(t'') \leq \tau_{\min}$. With some positive probability an oscillator i from the edge set ∂S fires at $t_e > t''$ and the pulse is received by all $k \in \mathtt{suc}_i$ at $t_r^k \in [t_e + \tau_{\min}, t_e + \tau_{\max}]$, and no other oscillator emits a pulse within $[t_e, t_e + \tau_{\max}]$. If $\phi_k(t_r^k) \in U_2 \cup U_3$ we apply Lemmas 1 and 2

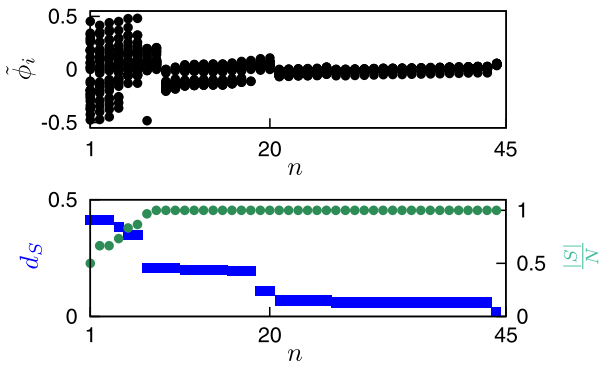

Fig. 8. An example of the synchronization process with, $|I| = 30$. On the top half we plot the phase positions at individual fire events t_n according to $\tilde{\phi}_i := (\phi_i + 0.5 \mod 1) - 0.5)$ for all $i \in I$. As time evolves the phases gather around 0 and thereby synchronize. On the bottom half we show the evolution of the diameter d_I and consider a maximal set S such that d_S satisfies (17). We see that as soon as the synchronization condition (17) is fulfilled for all oscillators $(S = I)$, d_S monotonically decreases.

and see $d_{ik}(t_r^{k+}) \leq (1/4) - \tau_{\max} - \tau_{\min}$. If $\phi_k(t_r^k) \in U_4 \cup U_5 \cup U_1$ we see with Lemma 1 $d_{ik}(t_r^{k+}) \leq 1/4$. Hence with Lemma 5 we have

$$d_{\mathrm{suc}_i \cup \{i\}} \left(t_r + \tau_{\max}^+\right) \leq \frac{1}{2} - \tau_\Delta. \tag{24}$$

This yields, defining $S' = S \cup \mathrm{suc}_i \cup i$

$$\begin{aligned} d_{S'} \left(t_r + \tau_{\max}^+\right) &\leq d_S \left(t_r + \tau_{\max}^+\right) \\ &\quad + d_{\mathrm{suc}_i \cup \{i\}} \left(t_r + \tau_{\max}^+\right) \\ &\leq \tau_{\min} + \frac{1}{2} - \tau_\Delta = \frac{1}{2} - \tau_{\max}. \end{aligned} \tag{25}$$

We augment S to S' and see that condition (17) has a positive probability to hold on $d_{S'}$ for all $t > t_r + \tau_{\max} > t''$. We hence repeat this argument for S' until (17) holds for d_I. Every assumption within this proof holds with some positive probability. Since we only need finitely many steps to reach $S = I$, the whole process has positive probability. ■

Theorem 1: Any self-organizing oscillator system with dynamics given by (2)–(7), with individual delays and connected dynamic networks as described in Section II-B1 and B2, synchronizes almost surely, i.e.,

$$\mathbb{P}\left[\lim_{t\to\infty} \max_{i,j\in I} d_{ij}(t) = 0\right] = 1. \tag{26}$$

Proof: Lemma 11 ensures a positive probability that for all elements in the system and for some point in time t_*, (17) and hence Lemma 10 holds. Thus, the probability that (17) does not occur within the time interval T_I is some $\beta < 1$ and hence for $n \in \mathbb{N}$ such time intervals, it is less or equal to β^n. This yields $\mathbb{P}[\lim_{n\to\infty} t_* \notin nT_I] = 0$ and hence (26). ■

Fig. 8 shows an example of such a chain of synchronizing events.

E. Limitations for Further Generalizations

Theorem 1 guarantees synchronization with probability 1. This statement is optimal in the following sense: We demonstrate via Examples 1 and 4 that a stronger statement cannot be made, via Example 3 how critical the requirements are and via Example 2 that a more general statement has to be weaker:

Example 1: Take a set of $N > 4$ oscillators on a static star graph, i.e., a central oscillator c is linked to any other oscillator in the system and no further links exist, hence for all $i \in I$ with $i \neq c$ we have for all t, $\mathrm{suc}_i(t) = \{c\}$. Assume $p_{\mathrm{send}} = 1$ and $\tau_{\min} = 0, \tau_{\max} \leq 1/8$. Furthermore we assume that at t_0 all phases are equally spaced with $\phi_c(t_0) = 0$. If no interactions happen we have for all fire events $t_{n+1} - t_n \leq 1/N$. After the first fire event we have $\phi_c(t_1) < (1/2) - \tau_{\max}$ and after the reception time $t_{r,1}$ we have $\phi_c(t_{r,1}^+) \leq (1/4) - \tau_{\max}$. At t_2 we have $\phi_c(t_2) \leq (1/4) - \tau_{\max} + (1/N) < 1/2$ and after the reception time $t_{r,2}$ $\phi_c(t_{r,2}^+) \leq (1/4) - \tau_{\max}$. Hence, for all $t > t_0$, we have $\phi_c(t) < (1/2)$. Therefore oscillator c will never fire, and no other oscillator than c adjusts. Hence synchronization does not emerge.

Example 1 shows that if we want to guarantee synchronization for a coupling strategy as proposed in (6) and (7) that works for all connected networks, we need $p_{\mathrm{send}} < 1$. Hence, the synchronization guarantee for arbitrary network topologies can only hold in a probabilistic sense.

Example 2: Assume a set I of oscillators with inhomogeneous phase rates, i.e., for all $i \in I$: $(d\phi_i/dt)(t) = \kappa_i$, with $\kappa_i \in [1 - \varepsilon, 1 + \varepsilon]$, $0 < \varepsilon \ll 1$. Assume $p_{\mathrm{send}} < 1$ and for a time $t > 0$, $d_I(t) = 0$. Due to the different phase rates and the probabilistic pulse emission, there is always a point in time $t' > t$, such that with positive probability $d_I(t') > 0$ holds.

Example 2 shows that a synchronization guarantee with probability 1 is infeasible. If we want to additionally consider heterogeneous phase rates the convergence statement would need to be relaxed.

Example 3: Assume homogeneous phase rates again but consider the case that the delays assumed to lie within $\tau_{\min}$ and $\tau_{\max}$ actually lie between different extremes $\tilde{\tau}_{\min}$ and $\tilde{\tau}_{\max}$. For a firing event of ϕ_i at time t' with $d_I(t') = 0$ and a receiving oscillator j, we get at the reception time $t_r > t'$:

1) if $\tilde{\tau}_{\max} > \tau_{\max}$ and $\tau_{ij} \in (\tau_{\max}, \tilde{\tau}_{\max})$ then $d_I(t_r^+) > 0$ which contradicts Lemma 7;
2) if $\tilde{\tau}_{\max} < \tau_{\max}$ then Theorem 1 holds;
3) if $\tilde{\tau}_{\min} < \tau_{\min}$ and $\tau_{ij} \in (\tilde{\tau}_{\min}, \tau_{\min})$ then $d_I(t_r^+) > 0$ which contradicts Lemma 7, see also Fig. 17 for illustration;
4) if $\tilde{\tau}_{\min} > \tau_{\min}$ then Lemma 9 does not hold.

All delay information except for 2) are hence critical to guarantee synchronization.

Example 3 shows that a certain knowledge about the delays in the system is necessary for the synchronization proof to work. However, despite the randomly distributed delays considered here, and in contrast to [14], [15] where uncertainty in the delay results in natural bounds for the minimal achievable phase separation this information here is sufficient to achieve full phase synchronization.

Moreover, as we will see in Section V, numerics show robustness of the synchronization process against deviations of the delay distribution from the assumed one.

Example 4: Take a set of three oscillators with the following graph properties: $\texttt{pre}_2 = \{1, 3\}$ and $\texttt{pre}_1 = \texttt{pre}_3 = \emptyset$. The network is weakly connected and has two sources. Since both oscillator 1 and 3 have no possible inputs, they operate as if isolated. Hence, it is impossible for them to synchronize.

Example 4 shows that it is not possible to synchronize all weakly connected networks. Hence, our assumption on strongly connected networks cannot be generalized further.

IV. Synchronization Speed

Our convergence proof gives a qualitative statement that synchrony is reached using the given PCO synchronization scheme. Its power lies in its generality as it is applicable to a wide range of systems with time-varying topology, unreliable pulse emission, and arbitrarily distributed transmission delays. Because of this generality, the proof does not provide precise statements for the time needed to achieve synchronization. Here we derive estimates for the speed of synchronization.

We define the synchronization time $T^{(\alpha)}$ as the time it takes a system to reach synchrony with a precision α, i.e.,

$$T^{(\alpha)} := \inf_t \{t \in \mathbb{R}_+ : d_I(t) \leq \alpha\}. \tag{27}$$

In general, this time depends on the network properties and individual realization of the dynamics, i.e., on the initial phase positions, the network topologies and their changes, the pulse propagation times and their stochastic emissions. Thus, a full analysis of this synchronization time is beyond the scope of this work. In the following we provide estimates on how fast the system synchronizes. We therefore concentrate on three network topologies:

- all-to-all connected graphs (A2A), where all units are connected with each other;
- undirected Erdós-Rēnyi random graphs (ERG), where a link between two nodes exists with probability p_{link} [46];
- undirected random geometric graphs (RGG), where nodes are randomly distributed, sampling from a uniform distribution on the unit square, and an undirected link between two nodes exists if the nodes are at Euclidean distance of at most r [47].

To compare the latter two network types we use the average node degree μ, given by $\mu = Np_{\text{link}}$ for ERGs and by

$$\mu = Nr^2\pi\left(1 - \frac{8}{3\pi}r + \frac{1}{2\pi}r^2\right) \tag{28}$$

for RGGs [48].

Starting from uniformly distributed initial phases, the synchronization condition (17) is generally not fulfilled and the system has to reach that condition first. In A2As and ERGs this step is fast and a few initial pulses are sufficient (cf. Fig. 8). Due to the coupling functions considered here a single pulse is typically sufficient to reduce the distance between the sending oscillator i and receiving one j below $d_{ij} \leq 1/2 - \tau_{\max}$. Hence, given a pulse sending probability of p_{send} and average number of μ receiving oscillators it approximately takes about $N/p_{\text{send}}\mu$ oscillators to cross the threshold in order to reach a state in which the synchronization condition holds and thus

$$T^{(1/2-\tau_{\max})} \propto \frac{N}{p_{\text{send}}\ \mu} = \frac{1}{p_{\text{send}}\ p_{\text{link}}}. \tag{29}$$

This time will further increase with the length of the minimal paths between any two nodes in the network. It will also depend on $1 - p_{\text{send}}$ as there are certain topologies that do not give rise to synchrony when $p_{\text{send}} = 1$, e.g., as discussed in Example 1. See also Fig. 13 and Section V-D below for a detailed analysis of those effects.

Once the synchronization condition (17) is reached the diameter d_I will only decrease. There are two factors that determine the speed of this process: First, if a pulse is received within the refractory period U_2 or by oscillators not in the boundary sets there is no change in the diameter. Let us call pulse reception events in which the diameter actually decreases *beneficial events* (compare Lemma 9). Note that by Lemma 1 at a pulse reception event there is an oscillator in U_2. Thus, the smaller the diameter the more likely it becomes that the entire set of oscillators is found in U_2 at pulse reception. The rate for a beneficial event thus is expected to scale with the current diameter, or alternatively the time Δt to the next beneficial event becomes inversely proportional to d_I

$$\Delta t \approx \frac{\beta}{d_I}, \beta \in \mathbb{R}. \tag{30}$$

Second, once the system encounters a beneficial event the magnitude Δd_I by which the diameter is decreased will also scale with d_I, i.e.,

$$\Delta d_I \approx \delta d_I \tag{31}$$

for some $0 < \delta < 1$. In total, we thus expect the diameter of the system to decay according to

$$\dot{\Delta d_I} \approx -\frac{\Delta d_I}{\Delta t} \approx -\delta d_I \frac{d_I}{\beta} = -\lambda d_I^2 \tag{32}$$

and solving this we find

$$\Delta d_I(t) \approx \frac{d_I(0)}{d_I(0)\lambda t + 1} \tag{33}$$

i.e., for large time periods the diameter decays algebraically as $(\lambda t)^{-1}$ where $\lambda = \delta/\beta$. This form well matches numerical simulations for the considered network topologies as shown in Fig. 9(a).

The constant λ depends on various network parameters: Note that if d_I is small, all oscillators will approximately fire with their intrinsic oscillation rate 1. The rate of beneficial events is then proportional to the number of pulses sent, i.e., to p_{send} and to the number of oscillators by which this pulse is reached, i.e., to μ. Following Lemma 1, pulses are not beneficial when received within the refractory period U_2. If the oscillators are close to synchrony $d_I < \tau_\delta$, for an oscillator j to adjust is

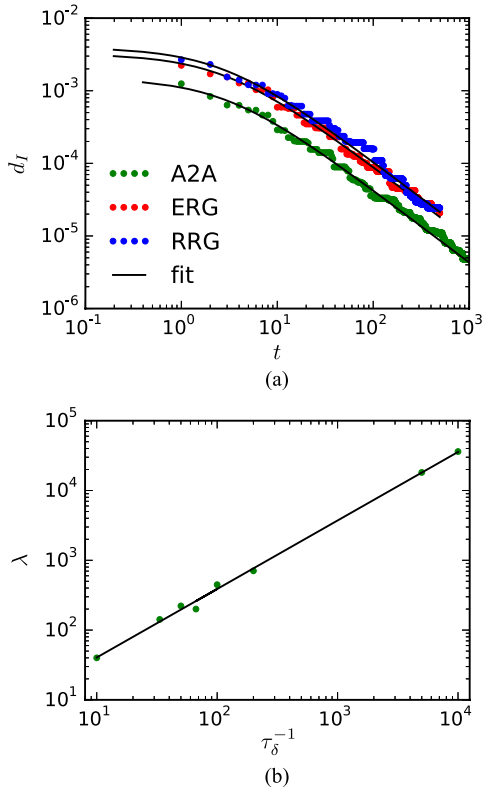

Fig. 9. Dynamics of the diamter d_I and scaling of λ with τ_δ^{-1}. (a) Diameter d_I as a function of time t. Lines are fits of (33) with parameter λ to the numerical data ($N = 100$, $\mu = N/2$) for the three different network topologies. (b) λ as a function of τ_δ^{-1} for an all-to-all network and linear fit (line) ($N = 100$).

only possible if this oscillator received a beneficial pulse within the current round of threshold crossings with $\phi_j > \tau_{\max}$ or $\phi_j < \tau_{\min}$. For small d_I the rate of beneficial pulses is small so that most of the pulses are actually received in the interval $[\tau_{\min}, \tau_{\max}] \subset U_2$. Thus the bigger this interval, the less likely an oscillator will receive a pulse in U_1 or U_3 necessary for a beneficial event. Thus, $\lambda \propto 1/\tau_\delta$. This scaling is shown if Fig. 9(b).

In total, we arrive at

$$\lambda \propto \frac{p_{\text{send}}\ \mu}{\tau_\delta}. \tag{34}$$

We also note that if the system is close to synchrony, i.e., $d_I < \tau_\delta$ and $d_I < \tau_{\min}$, it is more likely for an oscillator that is leading the group to trigger a beneficial event as it is for an oscillator that lags behind. These lagging oscillators are more likely to receive a beneficial pulse in U_1 while not having entered U_2 yet. In contrast, for pulses from lagging oscillators it is more likely to be received once the entire set of nodes is in the refractory period U_2.

V. Parameter Dependencies

The above convergence proof gives a qualitative statement that synchrony is reached using the given PCO synchronization scheme. We gave estimates on the synchronization speed in the previous section. Here we provide more details on the speed and robustness of the mechanism using numerical simulations.

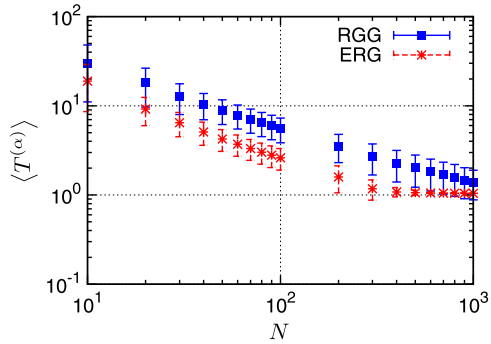

Fig. 10. Mean synchronization time decreases with increasing network size ($\mu = N/2$).

We focus on the synchronization time (27) and investigate how this time depends on network size, average node degree, dynamic network topology, synchronization precision, and signal emission probability. We also compare the synchronization behavior of our algorithm with that of Pagliari and Scaglione [7].

A. Definitions and Modeling Assumptions

Numerically we estimate the mean synchronization time by $\langle T^{(\alpha)} \rangle := (1/M) \sum_{i=1}^{M} T_i^{(\alpha)}$ where M is the number of realizations. In the figures we also indicate the standard deviation of this estimate via error bars.

The synchronization precision is set to $\alpha = 0.02$ and the signal emission probability to $p_{\text{send}} = 0.5$ unless mentioned otherwise. We use the phase update function (7) with $h_1 = 0.3261\phi + 0.0270$ and $h_2 = 0.46\phi + 0.54$ [see red line in Fig. 1(a)]. The delay is modeled to be randomly distributed uniformly within [0.02, 0.04]. A simulation runs for $2 \cdot 10^4$ cycles and we choose $M \geq 10^3$.

B. Effect of Network Size and Node Degree

Let us consider static networks first. Fig. 10 shows the mean synchronization time as a function of the number N of network nodes. For both network types, ERGs and RGGs, the larger N the faster synchrony is reached, representing a very favorable scalability property. In a network with $N = 100$ nodes, the synchronization time is below 10 cycles. We use $\mu = N/2$ in Fig. 10 which is consistent with the scaling behavior derived in (34). The synchronization speed saturates for larger N to a single cycle.

Even though the synchronization time decreases with increasing N, the number of fire events needed to reach that goal increases, as shown in Fig. 11.

Fig. 12 shows the mean synchronization time as a function of the average node degree μ for a network with 100 nodes. The synchronization time decreases with increasing μ, again consistent with the scaling in (34).

C. Effect of Pulse Emission Probability

Theorem 1 guarantees synchrony for arbitrary positive $p_{\text{send}} < 1$. We investigate a favorable parameter value that minimizes the number of fire events $\langle F^{(\alpha)} \rangle$ needed to achieve

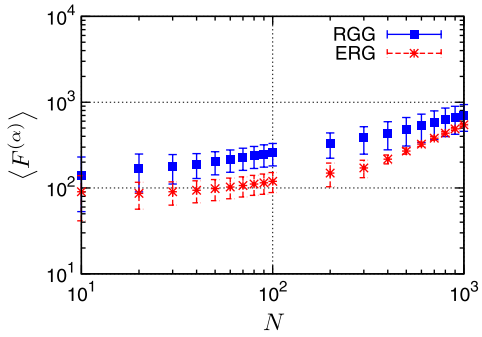

Fig. 11. Moderate increase of the mean number of total fire events $\langle F^{(\alpha)} \rangle$ to reach synchronization $d_I \leq \alpha = 0.02$ with increasing network size ($\mu = N/2$).

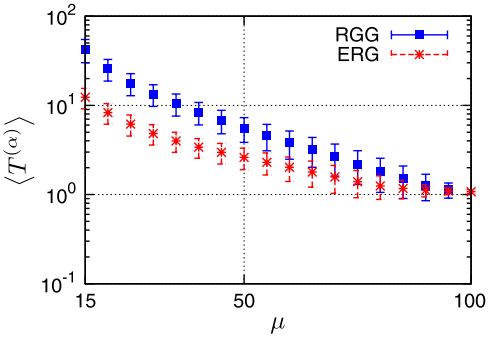

Fig. 12. Decreasing mean synchronization time $\langle T^{(\alpha)} \rangle$ with increasing average node degree μ ($N = 100$).

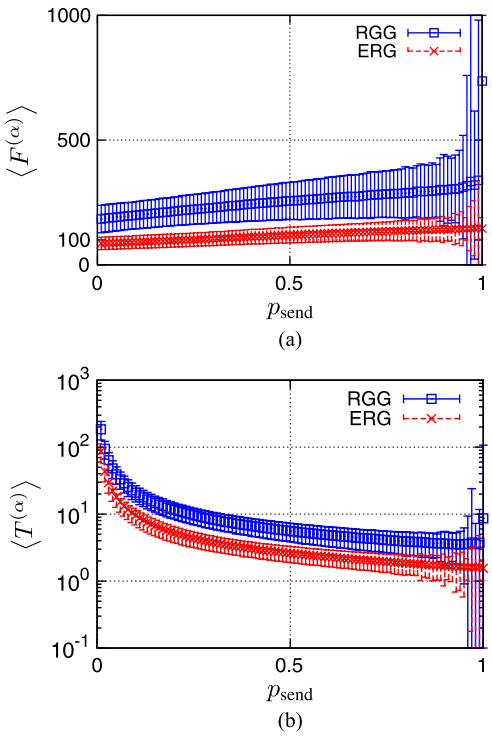

Fig. 13. Synchronization performance depending on the pulse emission probability p_{send}, in terms of: (a) mean fire events; and (b) mean synchronization time. For $p_{\text{send}} = 1$ we only consider simulations runs that synchronized (for all other parameters $p_{\text{send}} < 1$ all runs synchronized). ($N = 100$, $\mu = 50$).

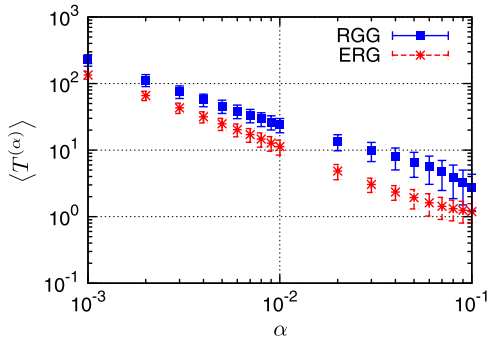

Fig. 14. Mean synchronization time as a function of the precision of synchronization α ($N = 100$, $\mu = 30$).

synchrony. This is important as the number of fire events relates to signaling overhead needed for synchronization, in terms of messages and energy. Fig. 13(a) shows the results. Interestingly, the smaller p_{send} the less fire events are needed. However, as shown in Fig. 13(b), this comes at the cost of increasing synchronization time, which follows our estimates (29) and (34). The optimal parameter setting for technical systems depends on the trade-off between the amount of energy spent on pulse emission and the need of fast convergence.

When p_{send} approaches 1, certain network topologies can increase the synchronization time as the probability for a chain of events that achieve the synchronization condition can become very unlikely (cf. Lemma 9 and Example 1). In Fig. 13 this effect becomes visible in the larger standard deviation for the synchronization time. For $p_{\text{send}} = 1$ not all simulation runs synchronized in the given maximal time frame again demonstrating the need for probabilistic fire events to achieve reliable synchronization.

D. Effect of Desired Precision in Synchronization

We terminate all simulations once the desired precision α is reached, i.e., $d_I < \alpha$. Fig. 14 shows how $\langle T^{(\alpha)} \rangle$ scales with decreasing α, confirming the algebraic decay as estimated in (33).

E. Effect of Dynamic Network Topologies

To explore the effect of dynamic network topologies on the synchronization process, we consider graphs that change every $\sigma_{\mathcal{G}}$ time units. In other words, a new network topology with the same statistical parameters for the random or random geometric graphs is created, every $\sigma_{\mathcal{G}}$ time units. We assume that a signal emitted by oscillator i at time t_n is received at oscillator j only if $j \in \mathtt{suc}_i(t)$ for all $t \in [t_n, t_n + \tau_{ij}]$.

Fig. 15 illustrates how the dynamics of the network topolgy influences the synchronization time. For quasi static networks $\sigma_{\mathcal{G}} \geq \langle T^{\alpha} \rangle$ the synchronization time is independent of $\sigma_{\mathcal{G}}$. If the network changes more frequently, as $\sigma_{\mathcal{G}}$ decreases, the synchronization time can significantly decrease. Dynamic networks can hence support synchronization. In Fig. 15(a), synchronization occurs faster in RGGs; in Fig. 15(b), synchronization occurs faster in both network types.

The decrease in $\langle T^{\alpha} \rangle$ stops once $\sigma_{\mathcal{G}} \approx 1$, i.e., the network topology changes on a time comparable to the rate with which

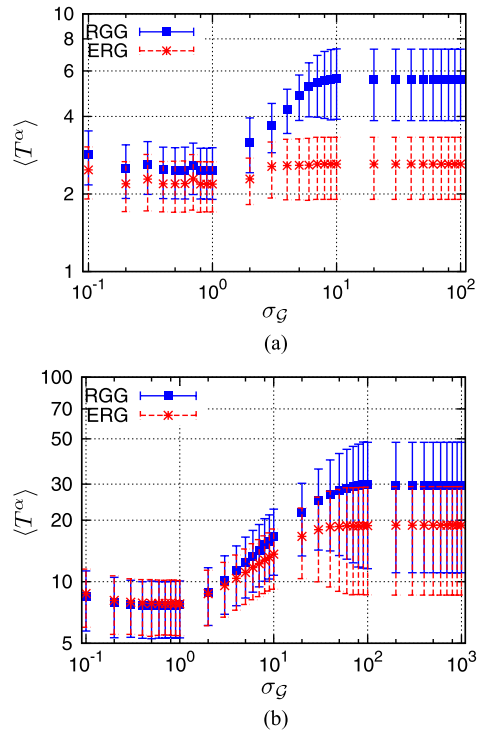

Fig. 15. Mean synchronization time $\langle T^\alpha \rangle$ as a function of the graph renewal time $\sigma_\mathcal{G}$, which is the length of the time intervals after which the network topology changes. (a) Networks with $N = 100$ and $\mu = 50$. (b) Networks with $N = 10$ and $\mu = 5$.

the oscillators cross the threshold. If the network topology is changing extremely fast, such that $\sigma_\mathcal{G} < \tau_{\max}$, the synchronization time increases sharply, as the probability for a signal not to be received increases.

The swift change in links increases the pool of pulse emission chains and hence the likelihood of finding a way to reach condition (17) (compare the constructive way in Lemma 11). Moreover, once this condition is reached, only beneficial events (cf. Section IV) will contribute in decreasing the diameter further and those beneficial events are more likely to occur for pulses emitted from oscillators close to the boundary. In particular, pulses from leading oscillators are most likely to trigger diameter decreases by pulling forward lagging oscillators. A changing network topology after each cycle ensures that such leading pulses are received by changing sets of lagging oscillators. This is process is most efficient after all oscillators have fired once, i.e., $\sigma_\mathcal{G} \approx 1$.

F. Robustness to Minimal Delay Assumptions

We assumed the delays to be distributed in a bounded interval with reoccurring delays arbitrarily close to the lower bound. In technical systems, it might not be possible to identify such a definite minimum delay. Hence, we here study the synchronization performance and robustness of the proposed algorithm if the theoretical assumed delays are within $[\tau_{\min}, \tau_{\max}]$ whereas the delays of the system are actually distributed within $[\tilde{\tau}_{\min}, \tau_{\max}]$ with $\tilde{\tau}_{\min} < \tau_{\min}$.

In Fig. 16 we show an example of a synchronization process when the assumption on the minimal delay is violated by

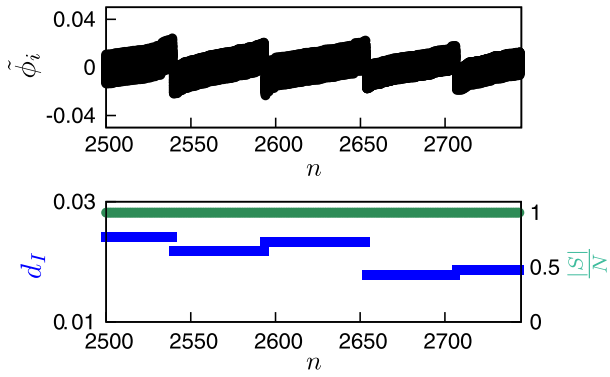

Fig. 16. Example of a convergence process with minimal transmission delay $\tilde{\tau} = 0.01$, whereas the theoretical delay is assumed to be $\tau_{\min} = 0.02$. We show a close up when a certain level of synchrony is achieved. Due to the inaccurate delay bounds that enter $H(\cdot)$ we see that d_I can increase. Note the small scale of fluctuations. Notation as in Fig. 8 ($N = 100$, $\mu = 30$, ERG).

the system. We observe that d_I fluctuates and can increase from time to time, hence (9) is no longer valid and synchronization to an arbitrary precision can not be guaranteed. Numerically, however, we find that a certain level of synchrony is still obtained. In Fig. 17(a) we see that for $\alpha \geq 5 \cdot 10^{-3}$ the synchronization time is showing similar behavior and that the mean synchronization time for $\tilde{\tau}_{\min} < \tau_{\min}$ is even a bit faster. For smaller α, however, the synchronization time for environments with $\tilde{\tau}_{\min} < \tau_{\min}$ increases much faster than that for the correct minimum possible delay. Fig. 17(b) supports the resilient behavior for mismatched parameters. The fraction ρ of simulation runs that synchronize is 1 as long as $\alpha \geq 5 \cdot 10^{-3}$, for lower α the resilient behavior is lost.

We interpret the beneficial impact of $\tilde{\tau}_{\min} < \tau_{\min}$ for $\alpha \in (0.0050.1]$ as follows. By moving the lower bound $\tilde{\tau}_{\min}$ below $\tau_{\min}$, the likelihood for delays around $\tau_{\min}$ increases (as it shifts from the border to the interior-assuming uniform distribution, cf. also Section IV). The improvement in probability decreases the time to reach condition (17). For $\alpha \leq 0.005$ we see the negative effects of inaccurate delay bounds, compare also Example 3.

G. Comparison With Pagliari–Scaglione Approach

We compare our work with that of Pagliari and Scaglione [7]. The authors did analytical and simulation studies on a PCO system with stochastic pulse reception but with less general system assumptions. For a comparison, we have to restrict our system settings by demanding that $\tau_{\min} = \tau_{\max} = 0.02$. The phase adjustment in [7] works as follows: Assume oscillator i receives a signal at time t then

$$\phi_i(t^+) = \begin{cases} \phi_i(t) & \phi_i(t) \leq \phi_{\text{ref}} \\ \min\left(1, a_1 \cdot \phi_i(t) + a_2\right) & \phi_i(t) > \phi_{\text{ref}} \end{cases} \tag{35}$$

with $a_1 = \exp(\varepsilon)$ and $a_2 = (\exp(\varepsilon) - 1)/(\exp(1) - 1)$. We use $\varepsilon_1 = 1$ and $\varepsilon_2 = 1 + 1/(Np_{\text{link}})$ as in [7]. Note that this algorithm was designed for stochastic pulse reception and positive probability for any link within the network. Here, we use arbitrarily connected and static networks, stochastic pulse

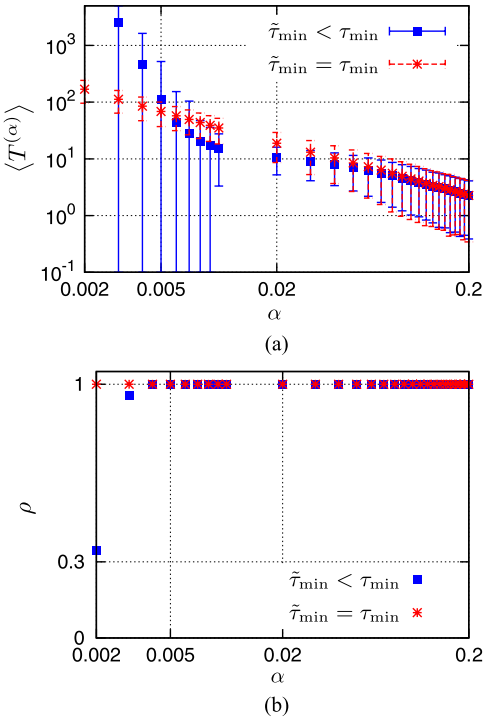

Fig. 17. The different synchronization performances if delays in practice ($\tilde{\tau}$) match or mismatch the theoretical ones (τ). (a) We plot the synchronization time for synchronizing simulation runs. (b) The fraction ρ of all simulations that synchronize shows that both parameter settings provide synchrony for $\alpha \geq 0.005$. For lower α the fraction drops significantly for mismatched parameters ($N = 10$, $\mu = 5$, $\tilde{\tau}_{\min} = 0.01$, ERG).

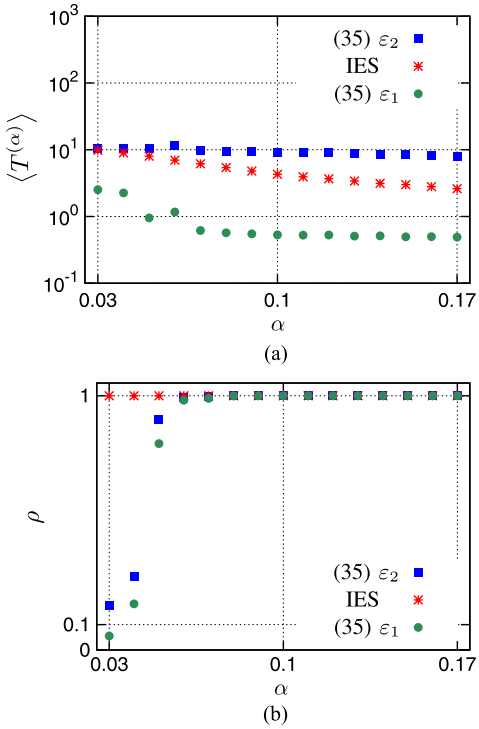

Fig. 18. Performance of the combined inhibitory and excitatory stochastic coupling scheme proposed in this paper (IES) in comparison to the algorithm of Pagliari and Scaglione in [7]. In (a), the synchronization time of all synchronizing simulation runs and in (b), the fraction of simulations that synchronize is shown. For readability the standard deviation in (a) is dropped. ($N = 10$, $\mu = 5$ ERG).

emission, and ensured pulse reception. The achievable close-to-synchrony state for this algorithm is bounded by ϕ_{ref} with $\phi_{\text{ref}} \geq 2\tau_{\max}$. Better synchronization than $\max_{ij} d_{ij} \leq \phi_{\text{ref}}$ is impossible in general. Fig. 18(a) compares the synchronization time for realizations that synchronize for different synchronization bounds α. The figure only depicts simulation runs that actually synchronized. The version with ε_1 synchronizes faster, the version with ε_2 synchronizes slower than the introduced algorithm. The parameter ε_1 refers to extreme coupling, which makes the algorithm fast but not robust.

Fig. 18(b) shows the fraction of simulations ρ that synchronize within the observation window of 20.000 cycles. For $\alpha < 0.06$, ρ decreases drastically, hence the Pagliari–Scaglione algorithm is not able to synchronize most networks under investigation. The synchronization method proposed here, however, still synchronizes all networks. The shown comparison is limited, however, it demonstrates the main improvement of the coupling scheme combining both inhibitory and excitatory coupling and stochastic pulse emission. It synchronizes arbitrary networks to arbitrary synchronization precision and any connected topologies. This convergence is proven for very general conditions and also works for individual random delays, a major difference to [7].

VI. Conclusion

In this paper, we introduced a class of update functions for pulse-coupled oscillators and showed their synchronizing properties. The proposed update function consists of excitatory and inhibitory parts together with a refractory period.

We prove that under the proposed coupling scheme pulse-coupled oscillators fully synchronize with probability 1. The synchronization is guaranteed for all of the following conditions: 1) in environments that experience nonnegligible delays, these delays may be constant or vary within an interval; 2) for arbitrary connected networks whose topology can even change dynamically in time; 3) on systems with probabilistic signal loss such as fading. These general system requirements are intended for making our theory applicable to real world environments.

In addition to our analytical results, which constitute the main contribution of this work, we further estimated how the speed in synchronization scales with the various system parameters and in addition used numerical studies to identify the following properties: 1) The synchronization algorithm scales well with growing network size. If sufficiently dense connected, a larger number of nodes speeds up the synchronization process. 2) For random geometric graphs, synchronization time is achieved faster if the network is dynamically changing. Changing the network topology faster than the intrinsic oscillation frequency of the network is however not improving the synchronization speed further. Hence, synchronization time is optimal if the network topology changes on intermediate timescales. 3) For the systems considered, energy efficiency can be improved by reducing the number of exchanged pulses and still achieve the desired synchronization level. A smaller

number of exchanged pulses is balanced by a larger expected time to synchrony. 4) The system is robust against delays outside of the considered range of delays.

These results highlight a number of advantages of the introduced algorithm and coupling scheme compared to previous work. The scheme is of low complexity and can be implemented in already existing slot synchronization strategies with finite synchronization words (cf. [6]). A testbed implementation recently made [49] supports the theoretical results of this article.

References

[1] C. S. Peskin, *Mathematical Aspects of Heart Physiology* ser. Courant Institute Lecture Notes, Courant Inst. Math. Sci., 1975, pp. 268–278.

[2] R. E. Mirollo and S. H. Strogatz, "Synchronization of pulse-coupled biological oscillators," *SIAM J. Appl. Math.*, vol. 50, no. 6, pp. 1645–1662, Dec. 1990.

[3] R. Mathar and J. Mattfeldt, "Pulse-coupled decentral synchronization," *SIAM J. Appl. Math.*, vol. 56, no. 4, pp. 1094–1106, Aug. 1996.

[4] Y.-W. Hong and A. Scaglione, "A scalable synchronization protocol for large scale sensor networks and its applications," *IEEE J. Sel. Areas Commun.*, vol. 23, no. 5, pp. 1085–1099, May 2005.

[5] G. Werner-Allen, G. Tewari, A. Patel, M. Welsh, and R. Nagpal, "Firefly-inspired sensor network synchronicity with realistic radio effects," in *Proc. ACM Conf. Embed. Netw. SenSys*, San Diego, CA, USA, Nov. 2005, pp. 142–153.

[6] A. Tyrrell, G. Auer, and C. Bettstetter, "Emergent slot synchronization in wireless networks," *IEEE Trans. Mobile Comput.*, vol. 9, no. 5, pp. 719–732, May 2010.

[7] R. Pagliari and A. Scaglione, "Scalable network synchronization with pulse-coupled oscillators," *IEEE Trans. Mobile Comput.*, vol. 10, no. 3, pp. 392–405, Mar. 2011.

[8] J. He, P. C. Cheng, L. Shi, J. Chen, and Y. Sun, "Time synchronization in WSNs: A maximum-value based consensus approach," *IEEE Trans. Autom. Control*, vol. 59, no. 3, pp. 660–675, Mar. 2014.

[9] W. Gerstner, "Rapid phase locking in systems of pulse-coupled oscillators with delays," *Phys. Rev. Lett.*, vol. 76, pp. 1755–1758, Mar. 1996.

[10] P. Goel and B. Ermentrout, "Synchrony, stability, and firing patterns in pulse-coupled oscillators," *Physica D*, vol. 163, pp. 191–216, 2002.

[11] A. Daliot, D. Dolev, and H. Parnas, "Self-stabilizing pulse synchronization inspired by biological pacemaker networks," in *Proc. Internat. Conf. Self-stabilizing Systems*, Jun. 2003, pp. 32–48.

[12] V. Klinshov and V. Nekorkin, "Synchronization of time-delay coupled pulse oscillators," *Chaos, Solitons Fractals*, vol. 44, pp. 98–107, 2011.

[13] S. Olmi, A. Politi, and A. Torcini, "Collective chaos in pulse-coupled neural networks," *Europhys. Lett.*, vol. 92, p. 60007, 2010.

[14] L. Lundelius and N. Lynch, "An upper and lower bound for clock synchronization," *Inf. Control*, vol. 62, pp. 190–204, Sep. 1984.

[15] H. Kopetz, *Real-time systems Design Principles for Distributed Embedded Applications*. Norwood, MA, USA: Kluwer, 2003.

[16] W. Kinzel, "On the stationary state of a network of inhibitory spiking neurons," *J. Comput. Neurosci.*, vol. 24, pp. 105–112, Feb. 2008.

[17] J. Friedrich and W. Kinzel, "Dynamics of recurrent neural networks with delayed unreliable synapses: Metastable clustering," *J. Comput. Neurosci.*, vol. 27, pp. 65–80, Aug. 2009.

[18] J. Klinglmayr, C. Kirst, C. Bettstetter, and M. Timme, "Guaranteeing global synchronization in networks with stochastic interactions," *New J. Phys.*, vol. 14, Jul. 2012, Art. no. 073031.

[19] Y. Wang, F. Núñez, and F. J. Doyle, "Increasing sync rate of pulse-coupled oscillators via phase response function design: Theory and application to wireless networks," *IEEE Trans. Control Syst. Technol.*, vol. 21, no. 4, pp. 1455–1462, Jul. 2013.

[20] J. Nishimura and E. J. Friedman, "Probabilistic convergence guarantees for type-ii pulse-coupled oscillators," *Phys. Rev. E*, vol. 86, Aug. 2012, Art. no. 025201.

[21] Y. Wang, F. Nunez, and F. Doyle, "Statistical analysis of the pulse-coupled synchronization strategy for wireless sensor networks," *IEEE Trans. Signal Process.*, vol. 61, no. 21, pp. 5193–5204, Nov. 2013.

[22] D. Buranapanichkit, N. Deligiannis, and Y. Andreopoulos, "Convergence of desynchronization primitives in wireless sensor networks: A stochastic modeling approach," *IEEE Trans. Signal Process.*, vol. 63, no. 1, pp. 221–233, Jan. 2015.

[23] A. T. Winfree, "Biological rhythms and the behavior of populations of coupled oscillators," *J. Theoret. Biol.*, vol. 16, no. 1, pp. 15–42, Jul. 1967.

[24] J. Buck, E. Buck, J. Case, and F. Hanson, "Control of flashing in fireflies. V. Pacemaker synchronization in *pteroptyx cribellata*," *J. Comput. Physiol. A*, vol. 144, no. 3, pp. 630–633, Sep. 1981.

[25] J. Klinglmayr and C. Bettstetter, "Self-organizing synchronization with inhibitory-coupled oscillators: Convergence and robustness," *ACM Trans. Autonom. Adapt. Syst.*, vol. 7, no. 3, p. 30, Sep. 2012.

[26] Y. Kuramoto, "Collective synchronization of pulse-coupled oscillators and excitable units," *Physica B*, vol. 50, pp. 15–30, 1991.

[27] U. Ernst, K. Pawelzik, and T. Geisel, "Synchronization induced by temporal delays in pulse-coupled oscillators," *Phys. Rev. Lett.*, vol. 74, no. 9, pp. 1570–1573, Feb. 1995.

[28] U. Ernst, K. Pawelzik, and T. Geisel, "Delay-induced multistable synchronization of biological oscillators," *Phys. Rev. E*, vol. 57, pp. 2150–2162, Feb. 1998.

[29] C. van Vreeswijk and H. Sompolinsky, "Chaos in neuronal networks with balanced excitatory and inhibitory activity," *Science*, vol. 274, pp. 1724–1726, 1996.

[30] A. Nischwitz and H. Gliinder, "Local lateral inhibition: A key to spike synchronization?" *Biol. Cybern.*, vol. 73, pp. 389–400, 1995.

[31] M. Timme and F. Wolf, "The simplest problem in the collective dynamics of neural networks: Is synchrony stable?" *Nonlinearity*, vol. 21, p. 1579, Jul. 2008.

[32] C. Kirst, T. Geisel, and M. Timme, "Sequential desynchronization in networks of spiking neurons with partial reset," *Phys. Rev. Lett.*, vol. 102, Feb. 2009, Art. no. 068101.

[33] C. Kirst and M. Timme, "Partial reset in pulse-coupled oscillators," *SIAM J. Appl. Math.*, vol. 70, pp. 2119–2149, 2010.

[34] A. Tyrrell, G. Auer, and C. Bettstetter, "Fireflies as role models for synchronization in ad hoc networks," presented at the *Int. Conf. Bio-Inspired Models Netw. Inf. Comput. Syst. (BIONETICS)*, Cavalese, Italy, Dec. 2006.

[35] A. Tyrrell, G. Auer, C. Bettstetter, and R. Naripella, "How does a faulty node disturb decentralized slot synchronization over wireless networks?" presented at the *IEEE ICC*, Cape Town, South Africa, May 2010.

[36] J. Nishimura and E. J. Friedman, "Robust convergence in pulse-coupled oscillators with delays," *Phys. Rev. Lett.*, vol. 106, no. 19, May 2011, Art. no. 194101.

[37] W. Wang and J. Slotine, "On partial contraction analysis for coupled nonlinear oscillators," *Biol. Cybern.*, vol. 92, no. 1, pp. 38–53, 2004.

[38] A. Pogromsky, G. Santoboni, and H. Nijmeijer, "Partial synchronization: From symmetry towards stability," *Physica D*, vol. 172, no. 2, pp. 65–87, 2002.

[39] S. Shafi, M. Arcak, M. Jovanovic, and A. Packard, "Synchronization of diffusively-coupled limit cycle oscillators," *Automatica*, vol. 49, no. 12, pp. 3613–3622, 2013.

[40] R. Sepulchre, "Consensus on nonlinear spaces," *Annu. Rev. Control*, vol. 35, no. 1, pp. 56–64, 2011.

[41] A. Hamadeh, G. Stan, R. Sepulchre, and J. Goncalves, "Global state synchronization in networks of cyclic feedback systems," *IEEE Trans. Autom. Control*, vol. 57, no. 2, pp. 478–483, Feb. 2012.

[42] P. Sacre and R. Sepulchre, "Sensitivity analysis of oscillator models in the space of phase-response curves: Oscillators as open systems," *IEEE Control Syst.*, vol. 34, no. 2, pp. 50–74, Apr. 2014.

[43] F. Dörfler and F. Bullo, "Synchronization in complex networks of phase oscillators: A survey," *Automatica*, vol. 50, no. 6, pp. 1539–1564, 2014.

[44] M. Timme, F. Wolf, and T. Geisel, "Coexistence of regular and irregular dynamics in complex networks of pulse-coupled oscillators," *Phys. Rev. Lett.*, vol. 89, no. 25, Nov. 2002, Art. no. 258701.

[45] P. Ashwin and M. Timme, "Unstable attractors: Existence and robustness in networks of oscillators with delayed pulse coupling," *Nonlinearity*, vol. 18, pp. 2035–2060, 2005.

[46] P. Erdós and A. Rēnyi, "On random graphs," *Publ. Math. Debrecen*, vol. 6, pp. 290–297, 1959.

[47] M. Penrose, *Random Geometric Graphs*. London, U.K.: Oxford Univ. Press, 2003.

[48] C. Bettstetter, *Mobility Modeling, Connectivity, and Adaptive Clustering in Ad Hoc Networks*. Munich, Germany: Herbert Utz Verlag, 2004.

[49] G. Brandner, U. Schilcher, and C. Bettstetter, "Firefly synchronization with phase rate correction and its experimental analysis in wireless systems," *Comput. Netw.*, vol. 97, pp. 74–87, 2016.

Johannes Klinglmayr received the Dipl.-Ing. degree in technical mathematics from the Technical University of Vienna, Vienna, Austria, in 2007, the M.A. degree in applied mathematics from the University of Michigan, Ann Arbor, MI, USA, in 2008, and the Dr. techn. degree in information technology from the University of Klagenfurt, Klagenfurt, Austria, in 2013.

He was with the University of Klagenfurt and Lakeside Labs, Klagenfurt, from 2008 to 2013. From 2009 to 2013, he was a repeating Visiting Researcher with the Max-Planck Institute for Dynamic and Self-Organization, Göttingen, Germany. He has been a Senior Engineer at the Linz Center of Mechatronics, Linz, since 2014. His research focus is on self-organization and interdisciplinary applications.

Christian Bettstetter (S'98–M'04–SM'09) received the Dipl.-Ing. degree, in 1998, and the Dr.-Ing. degree (*summa cum laude*), in 2004, both in electrical and computer engineering from the Technische Universität München (TUM), Munich, Germany.

He was a Staff Member with the Communications Networks Institute, TUM, until 2003. From 2003 to 2005, he was a Senior Researcher with DOCOMO Euro-Labs. Since 2005, he has been a Professor and Head of the Institute of Networked and Embedded Systems, University of Klagenfurt, Austria. He is also Scientific Director and Founder of Lakeside Labs, Klagenfurt, a research cluster on self-organizing networked systems. He coauthored the textbook GSM:Architecture, Protocols and Services (Wiley).

Mr. Bettstetter received Best Paper Awards from the IEEE Vehicular Technology Society and the German Information Technology Society (ITG).

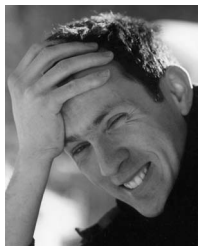

Marc Timme studied physics and mathematics in Wrzburg, Stony Brook, New York, NY, USA, and Göttingen. After a master's degree (1998, Stony Brook) and a Doctorate in Theoretical Physics (2002, Göttingen), he worked as a postdoctoral researcher at the MPI for Flow Research from 2003.

After work as a Research Scholar at the Center of Applied Mathematics, Cornell University (USA), he became head of the research group Network Dynamics of the Max Planck Society in December 2006. He is a founding member of the Bernstein Center for Computational Neuroscience Göttingen and on the steering committee of the International Max Planck Research School for Physics of Biological and Complex Systems. Since 2009, he has been an Adjunct Professor at the University of Göttingen, and as of 2016, also a Visiting Professor at the TU Darmstadt. His research interests include the nonlinear collective dynamics of networked systems in biology, physics, and engineering, and their functional and computational capabilities.

Dr. Timme was awarded the Otto Hahn Medal (2002), the Berliner Ungewitter Award (2003), as well as invited as Research Fellow of the National Academy of Italy (2009).

Christoph Kirst studied mathematics and physics at the Universities of Göttingen, Berlin, Oxford, U.K., and Cambridge, U.K. He received the Certificate of Advanced Study in Mathematics (Part III, Cambridge), the Dipl.-Phys. degree (Göttingen), and a Dr.rer.nat. in theoretical physics (Max Planck Institute for Dynamics and Self-Organization, Göttingen).

After a postdoctoral stay at the LMU/Bernstein Center for Computational Neuroscience in Munich, he now is a Fellow for physics and biology at the Rockefeller University New York City (USA). His research focusses on communication and dynamics in networks with applications to artificial and biological systems.